Synchronized Triple Bias-Flip Circuit for Piezoelectric Energy Harvesting Enhancement: Operation Principle and Experimental Validation

Yuheng Zhao and Junrui Liang
School of Information Science and Technology
ShanghaiTech University, Shanghai 201210, China
Emails: {zhaoyh, liangjr}@shanghaitech.edu.cn

***Abstract*—The power conditioning circuit plays an important role in a piezoelectric energy harvesting (PEH) system. Sophisticatedly designed circuit can increase the harvesting capability by several times. The synchronized multiple bias-flip (SMBF) model generalizes the performance of existing interface circuits and offers prospect for future circuit evolution. Among all ideal SMBF derivatives, the parallel synchronized triple bias-flip (P-S3BF) circuit makes the best compromise between cost and effectiveness. This paper introduces a practical implementation of P-S3BF. It is realized by an inductive current-routing network, which is controlled by six MOSFET switches. The steady-state operation principle towards PEH enhancement is analyzed in detail. The transient behavior is also illustrated for highlighting the adaptive feature of the new circuit. Both theoretical and experimental results show that, under the same harmonic displacement excitation, the prototyped P-S3BF circuit can increase the maximum harvested power by 24.5% compared to the cutting-edge parallel synchronized switch harvesting on inductor (P-SSHI) circuit, and 287.6% compared to the standard bridge rectifier circuit.**

I. Introduction

The energy harvesting technologies have been extensively studied for more than a decade, in order to explore the self-powering solutions for distributed wireless sensor networks (WSNs) and portable devices [1], [2]. These solutions enable the future devices to power themselves by scavenging the energy from their ambiance. Piezoelectric transducers can be utilized to harvest the energy associated with ambient vibration. The harvested power of piezoelectric energy harvesting (PEH) system ranges from μW to mW level, which is suitable for some WSN applications. The power conditioning circuit converts the output ac from the PEH transducer into usable dc for powering electronics such as sensors, processors, etc. In the meanwhile, it intervenes the electromechanical conversion from the electrical side, such that can increase the harvesting capability. It was reported that sophisticatedly designed interface circuits can enhance the energy harvesting capability (maximum output power) by several times [3]. Therefore, the pursuit of more capable PEH interface circuits is one of the emphases in the research of PEH technology.

II. PEH Power Conditioning

A. Principle

To focus on the harvesting capability of the circuit, its effect on mechanical dynamics is neglected, which can be achieved with constant displacement excitation of the structure. Given such condition, a piezoelectric structure can be simply modeled as an ideal current source i_{eq} in parallel with the piezoelectric capacitance C_p and a leakage resistance R_p, which summarizes the effect of dielectric loss, as shown in Fig. 1(a). i_{eq} is proportional to the vibration velocity $\dot{x}$. The working frequency of piezoelectric structure ranges from several Hz for large structure to several kHz for MEMS structure, which is relative very low compared to most switching power electronics. The $\omega C_p R_p$ constant is usually much larger that unity. Therefore, R_p is large enough to be neglected in the parallel network unless the magnitude of v_p, the voltage across C_p, is boosted to a much higher level.

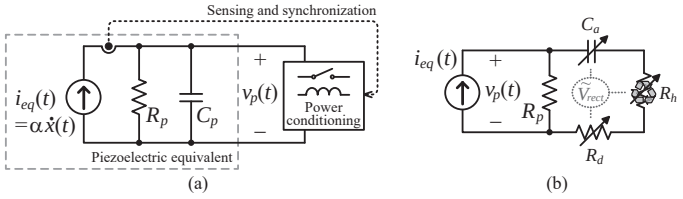

Fig. 1. Principle of PEH power conditioning. (a) Schematics. (b) Equivalent impedance model [4].

The objectives of PEH power conditioning are in two folds. One is for ac-to-dc conversion. The other is for harvested power enhancement by intervening the mechanical-to-electrical power conversion, which happens in the piezoelectric transducers. Such task might be achieved by making large voltage across the piezoelectric output electrodes, i.e., v_p in Fig. 1, in phase with the current i_{eq}.[1] Conventional power factor correction (PFC) circuit can hardly handle this task, due to the fact that the compensatory inductance is up to several hundred Henry. Instead of using the conventional PFC circuit, most existing solutions take advantage of the low frequency feature of mechanical vibration and capacitive output impedance of the piezoelectric device. Power electronics take actions sparsely only when i_{eq} or its mechanical counterpart, the vibration velocity $\dot{x}$, crosses zero.

The combined effect of C_p and the power conditioning

[1]Making large v_p is an essential, but not sufficient, condition. Refer to [4] for the whole story.

978-1-5090-0737-0/16/$31.00 ©2016 IEEE

circuit can be further modeled with an equivalent impedance model, as shown in Fig. 1(b) [4]. In the impedance model, R_h and R_d denote the effects of energy harvesting and dissipation in an interface circuit, respectively; C_a is an accompanied reactive component.

B. SBF interface circuits

The synchronized bias-flip (SBF) interface circuits are the most extensively studied circuit family for PEH enhancement. The idea is to instantaneous change the v_p polarity according to that of i_{eq}. It can be achieved because the response of electrical circuit is much faster than that of mechanical structure. Considering the internal capacitance C_p, the most energy efficient way to make instantaneous change to voltage polarity across C_p is to connect an external inductor L_i to C_p and utilizing the under-damped transient response of the LC circuit. The voltage change is maximized with lowest energy effort when the connecting time equals to half of an LC cycle, i.e., $\pi\sqrt{L_iC_p}$ [3], [4]. Such instantaneous voltage change is called (voltage) "flip". And "bias" in SBF refers to the reference voltage of the flipping action (usually a dc source connected in series with the LC circuit).

The synchronized switch harvesting on inductor (SSHI) is one of the earliest proposed and most popular SBF circuits. By only utilizing one passive (energy extracting) bias-flip action, SSHI can increase the harvested power by several folds [3], compared to the bridge rectifier, which is usually taken as the benchmark for harvested power comparison. Moreover, the state-of-the-art research shows that the harvesting capability can be further improved by taking active (energy injecting) bias-flip intervention, i.e., pumping a suitable amount of energy into the system at a suitable instant, in order to gain more return [5], [6].

Based on the evolutionary history of SBF circuits, Liang proposed a general synchronized multiple bias-flip (SMBF) model summarizing the principle of existing SBF circuits and also providing prospect for future circuit development [4]. The harvesting capabilities of parallel- and series-SMBF circuits are expressed as follows

$$\tilde{R}_{harv,\text{P-SMBF}} = \frac{M}{\pi}\frac{1-\gamma}{1+\gamma} + 1; \tag{1}$$

$$\tilde{R}_{harv,\text{S-SMBF}} = \frac{M}{\pi}\frac{1-\gamma}{1+\gamma}, \tag{2}$$

where γ is the voltage flipping factor, M is the number of synchronized bias-flip actions. From (1) and (2), it can be concluded that, with a fixed γ, which is determined by the quality factor of the LC circuit, the harvesting capability can be further enhanced beyond the state of the art by sophisticatedly carrying out more bias-flip actions at every synchronized instant, i.e., increasing the number M in (1) and (2).

III. P-S3BF Interface Circuit

The SMBF model has only provided a theoretical forecast of future PEH circuit development. Practical implementation of the multiple bias-flip actions is an issue. Some S-S2BF solutions (usually referred as pre-bias or pre-damping solutions) require pre-charged dc voltage sources for realizing the well-organized bias-flip actions [6], which is not self-adaptive under different vibration conditions. From the observation of the intermediate and bias voltages under optimal harvesting conditions (Fig. 11 in [4]), the most cost-effective solutions are P-S1BF (an alias of P-SSHI), P-S3BF, P-S5BF, etc., because they can achieve the best harvesting capability by making full use of 0, 1, 2, etc. adaptive voltage sources, respectively. In this paper, we introduce the implementation and operation of the self-adaptive P-S3BF interface circuit.

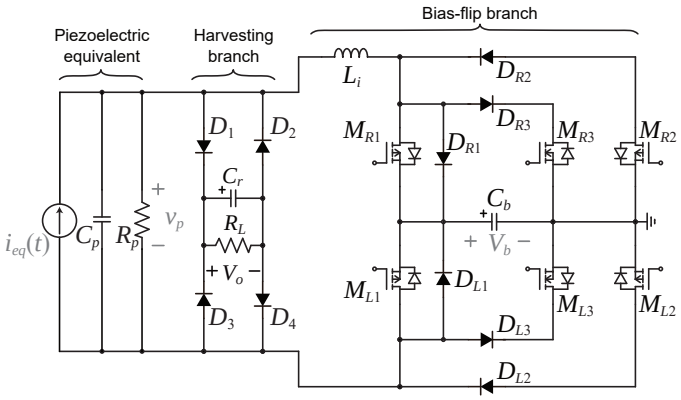

Fig. 2. P-S3BF interface circuit (need revision: larger font, specify the internal components inside the piezo).

From the optimal bias-flip (OBF) strategy derived based on the SMBF model [4], optimal P-S3BF requires three bias voltages, i.e., $-V_b$, 0, and V_b. Since zero volt just means short circuit, $-V_b$ and V_b are symmetric with respect to zero, the three bias voltages can be realized by using only one auxiliary voltage source, i.e., negative connection, short circuit, and positive connection. On the other hand, under the optimal condition, the energy income and expenditure of the bias voltage source balance in each synchronized instant, which means that the bias source need not to provide additional energy for carrying out the triple bias-flip actions. So general speaking, P-S3BF makes the best compromise between circuit complexity and harvesting capability.

Practical circuit topology of P-S3BF is shown in Fig. 2. The circuit is composed of two shunt branches: one for bias-flip actions and the other for energy harvesting. In the bias-flip branch, six MOSFET switches and six diodes form the current-routing network; the inductor L_i has the same purpose as that in SSHI, i.e., to form an under-damped switching LC circuit. The harvesting branch is just a convectional bridge rectifier for the ac-dc conversion.

A. Steady-State Operation

The detailed operation principle of P-S3BF is illustrated in Fig. 3. When the equivalent current $i_{eq}(t)$ crosses zero, three different current paths are formed successively in the bias-flip branch for rapidly flipping $v_p(t)$ for three times with respect to the dc bias reference voltages V_b, 0, and $-V_b$, respectively.

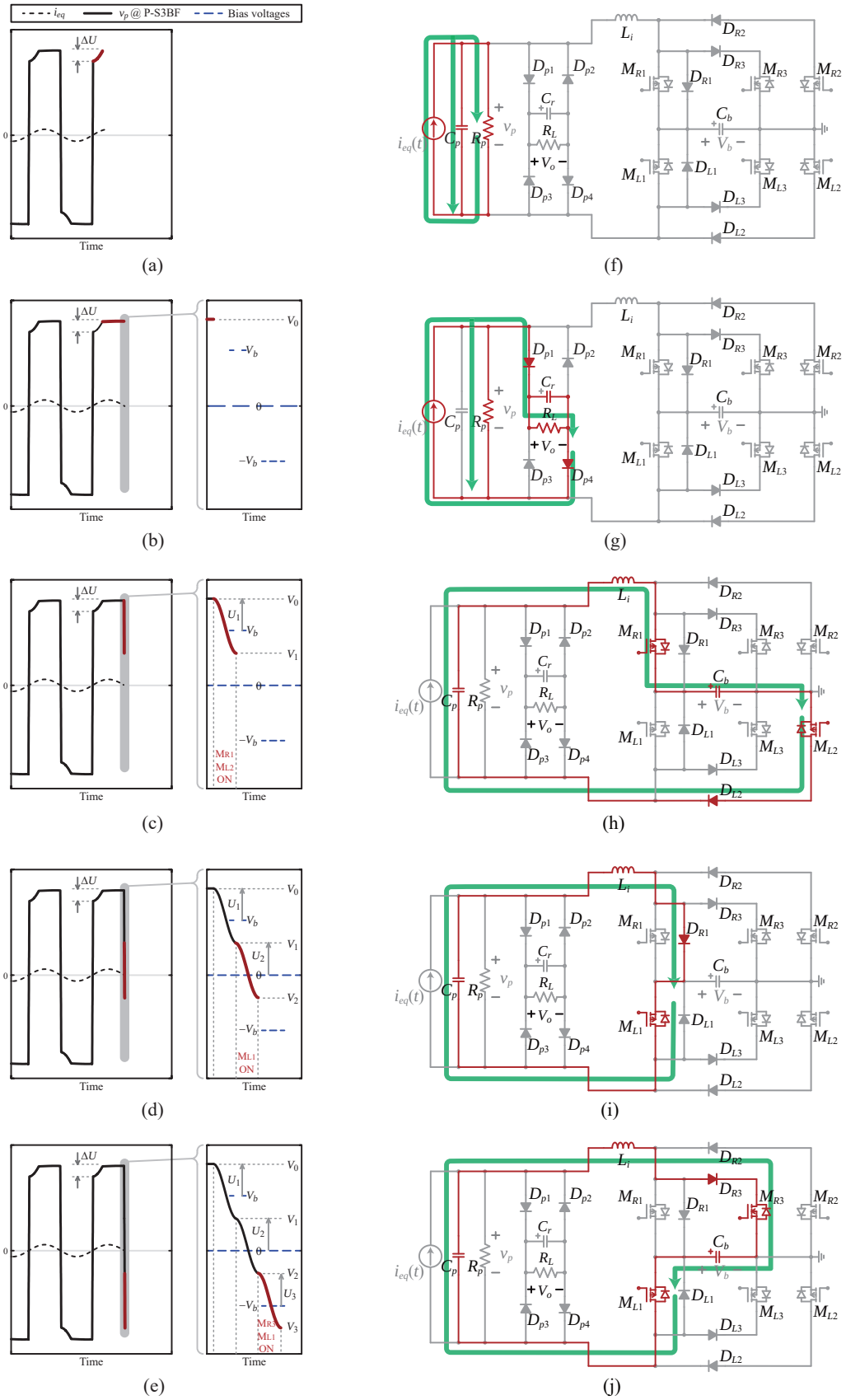

Fig. 3. The working phases of P-S3BF in half of a vibration cycle. (a)–(e) Waveforms. (f)–(j) Circuit operations. (a) and (f) Open circuit. (b) and (g) Constant voltage. (c) and (h) The first bias flip. (d) and (i) The second bias flip. (e) and (j) the third bias flip.

Such actions drive the piezoelectric voltage $v_p(t)$ towards a more opposite value in the most energy efficient manner. The three paths share the same inductance. The switch-on time is the same. Therefore, the three bias-flip actions have the same flipping factor. The working phases in a half vibration period are described as follows:

1) Open circuit: This phase starts right after the last upstairs actions. During this phase, the bias-flip and harvesting branches are blocked. C_p is charged by positive i_{eq}. Therefore, v_p the voltage across C_p rises from the initial value $-V_3$ until it arrives at V_0, as shown in Fig. 3(a).

2) Constant voltage (harvesting): In this phase, the diode bridge is conducted. i_{eq} flows into the harvesting branch. Since $C_r \gg C_p$, v_p is clamped at V_0, as shown in Fig. 3(b). The energy income from the current source i_{eq} in this phase balances with the energy consumed by the dc load R_L in a half vibration cycle.

3) The first bias flip: This phase starts at the positive-to-negative zero-crossing point of i_{eq}. In this phase, only M_{R1} and M_{L2} are turned on. The charge in C_p flows through a much larger C_b until v_p reach its first peak. The current direction is confined by D_{L2}; therefore, the current flows unidirectionally and it stops after half an LC cycle. The reference voltage of this bias-flip action is V_b. C_b absorbs energy from C_p during this phase.

4) The second bias flip: This phase follows the first bias-flip action. In this phase, only M_{L1} is turned on. The current through C_p is confined by D_{R1} in the same direction as the first bias-flip action did. The charge stored in C_p flows through the zero voltage reference. v_p flips from positive to negative. In this phase, there is no energy change in C_b.

5) The third bias flip: This phase follows the second bias-flip action. Only M_{L1} and M_{R3} are turned on. The current flow is confined in the same direction by D_{R3}. The reference voltage of this bias-flip action is $-V_b$. It drives v_p to a more negative value by injecting a specific amount of energy from C_b to C_p.

The bias-flip actions in the last three phases carry out the downstairs shape voltage migration for v_p. After the aforementioned five phases, there are another five counterpart phases in the rest half cycle. The last three out of the five carry out the upstairs shape voltage migration for v_p likewise. It is worth noting that, in steady-state, the energy absorbed by C_b in the first bias flip equals to that injected by C_b to C_p in the third bias flip. Moreover, the energy in C_b does not change during the second bias-flip action. Therefore, under steady state, C_b is energy neutral.

B. Harvested Power

The P-S3BF interface circuit is nonlinear, because it consist of bridge rectifier and MOSFET switches. The concept of impedance is used in conventional linear ac circuit analysis for showing the magnitude and phase relations between two sinusoidal variables. In order to use the impedance concept for analyzing P-S3BF, an assumption is made that the influence of high order harmonics caused by the harvesting circuit is much smaller than that of the fundamental harmonic. Under such assumption, the equivalent impedance of the circuit is decided by the fundamental harmonic of v_p and the sinusoidal i_{eq}. According to the formula provided in [7], the equivalent impedance of the combination of C_p and P-S3BF circuit can be derived as follows

$$\begin{aligned} Z_e(j\omega) =& R_d + R_h - j(\omega C_a)^{-1} \\ =& \frac{1}{\pi\omega C_p}\left\{\left[6\frac{1-\gamma}{1+\gamma}(1-\cos\theta)+\sin^2\theta\right]\right. \\ &\left. + j(\sin\theta\cos\theta-\theta)\right\}, \end{aligned} \tag{3}$$

where ω is the vibration angular frequency; θ is the phase angle of the open-circuit phase, which is related to the rectified voltage across C_r. In the total $Z_e(j\omega)$, the harvesting component R_h is the ac equivalent counterpart of the dc load R_L, which can be expressed as follows

$$R_h = \frac{2}{\pi\omega C_p}\left[\frac{2-\gamma}{1+\gamma}(1-\cos\theta)-\tilde{V_F}\right](1+\cos\theta), \tag{4}$$

where $\tilde{V_F} = V_F/V_{oc}$ is the normalized forward voltage drop of a diode. According to the topological relation shown in Fig. 1(b), the harvested power can be calculated as follows

$$P_h = \frac{R_h}{2}\left|\frac{I_{eq}R_p}{Z_e+R_p}\right|^2, \tag{5}$$

where I_{eq} is the magnitude of the equivalent current source i_{eq}, which is proportional to the vibration velocity.

C. Transient Performance and Adaptivity

One of the significant features of the proposed solution is that the dc bias voltage V_b provided by the capacitor C_b is

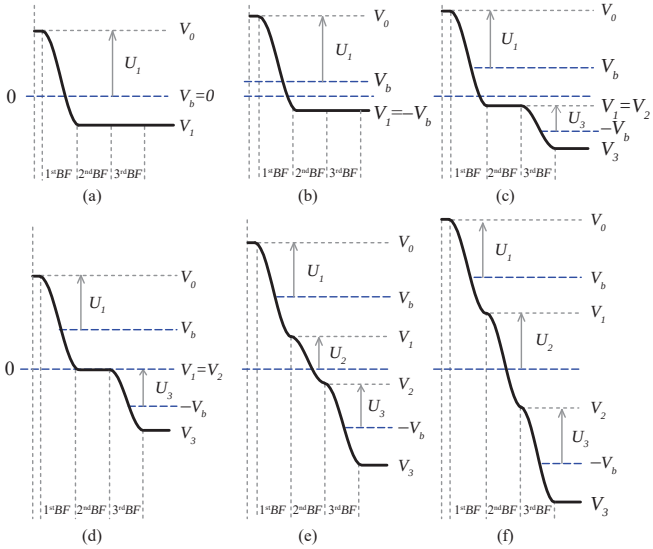

Fig. 4. Transient waveforms of P-S3BF in the synchronized (downstairs) instant. (a) Single BF ($V_1 < -V_b$). (b) Critical point between single and double BFs ($V_1 = -V_b$). (c) Double BFs ($-V_b < V_1 < 0$). (d) Critical point between double and triple BFs ($V_1 = 0$). (e) Triple BFs ($0 < V_1 < V_b/(1-\gamma)$). (f) Steady-state triple BFs ($V_1 = V_b/(1-\gamma)$).

self-adaptive. Given the specific current routing restrictions, C_b can be charged up from zero by the piezoelectric source at start-up; it can also be charged or discharged to a new level when vibration goes up or down, respectively.

When the interface circuit begins to work, there is no energy stored in C_b and thus V_b equals to zero. At the synchronized instant, v_p is flipped to the opposite sign after the first bias-flip action, such that the second and third current paths are blocked by the current routing diodes. There is only one BF action, as shown in Fig. 4(a). After this, C_b is purely charged at every synchronized instant until V_1 reaches the first critical point $-V_b$, as shown in Fig. 4(b). As V_b keeps rising, in the range of $-V_b < V_1 < 0$, the third BF action is activated (the second current path is still blocked), as shown in Fig. 4(c). In this stage, C_b is charged in the first BF and discharged in the third one. Since the voltage drop in the first action is larger than that in the third one, the net energy input to C_b is positive. Therefore, V_b keeps rising until V_1 reaches the second critical point zero, as shown in Fig. 4(d). As V_b keeps rising, in the range of $V_1 > 0$, the second BF action is activated, as shown in Fig. 4(e). The C_b stops charging and the voltage V_b becomes stable only when the voltage changes in the first and third bias-flip actions are the same. Under steady state operation, we have $V_1 = V_b/(1-\gamma)$.

Thanks to the dynamic energy balance of C_b, an adaptive bias voltage source V_b is achieved. In each synchronized instants, C_b absorbs energy from C_p in the first BF action and returns energy to C_p in the third BF action. If v_p increases beyond its current steady-state magnitude due to external perturbation (increase of vibration level or increase of electrical load R_L), the stroke of the first BF action becomes larger than that of the third on, i.e., $V_0 - V_1 > V_2 - V_3$. Since the energy absorbed by and return from C_b is given by

$$E_{in} = C_p(V_0 - V_1)V_b, \tag{6}$$

$$E_{out} = C_p(V_2 - V_3)V_b, \tag{7}$$

the unbalanced energy flow will charge C_b up until the net energy input becomes zero. On the other hand, when v_p drops below its current steady-state magnitude, the voltage change of the third bias-flip action will be larger than that of the first one; therefore, C_b will discharge until it arrives at the new energy equilibrium.

The self-adaptive feature ensures that the voltage is properly flipped with respect to the suitable dc bias voltages, regardless of the changes on vibration level or electrical loading condition. Moreover, it should be noted that smaller C_b helps faster arrival at the steady state. However, if C_b is too small, say, approaches the capacitance of C_p, it might fail to provide constant dc voltage towards stable triple BFs operation.

IV. Experiment

Fig. 5 shows the experimental setup. The main mechanical structure is an aluminum cantilever beam, which is excited by a shaker. Two piezoelectric patches are bonded near the fixed end of the beam. One patch is for energy harvesting and the other is for displacement sensing. For generating the synchronized switch control in P-SSHI or P-S3BF, an electromagnetic (EM) sensor, which is composed of a coil and a pair of permanent magnets, is employed to sense the relative velocity between the cantilever beam and the vibrating base. The permanent magnet serves as a proof mass, which can both lower the natural frequencies and increase the displacement of the free end at the same time. When the output voltage of the coil crosses zero, which is proportional to the relative velocity of the beam and i_{eq}, the micro-controller (MCU) is then triggered to drive the MOSFETs with specific sequences as shown in Fig. 3. In order to prevent noise in the EM sensor from accidentally triggering the MCU, a low-pass-filter (LPF) is connected between the EM sensor and the MCU. The parameters of the piezoelectric structure, i.e. C_p and R_p, are identified from measurement results. The prototyped P-S3BF circuit is shown in Fig. 6. Detailed mechanical and electrical specifications are listed in Table I and II, respectively.

Experiments are carried out for obtaining the harvested power P_h under constant magnitude harmonic displacement excitation. Three interface circuits including the standard bridge rectifier circuit (SEH), P-SSHI, and P-S3BF are con-

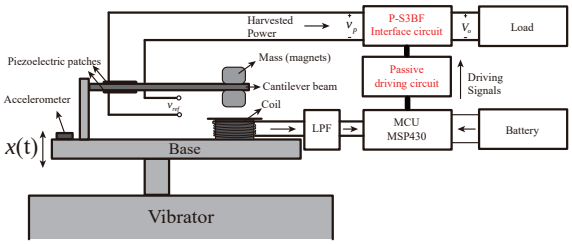

Fig. 5. Experimental setup.

TABLE I
Mechanical Specifications

Parameters	Value or model
Piezoelectric patch (PZT - 5)	$20.0 \times 20.0 \times 0.1$ (mm^3)
Cantilever beam (Aluminum)	$90.0 \times 20.0 \times 1.0$ (mm^3)
R_p	1.06 MΩ
C_p	28.42 nF
f_0	24.9 Hz
V_{oc}	15 V

TABLE II
Electrical Specifications

Parameters	Value or type
Schottky diodes	SS16
MOSFETs	Vishay Si4590DY
L_i	47 mH
C_r	10 μF
C_b	4.7 μF
γ	-0.7

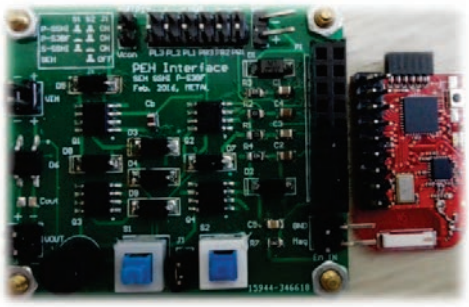

Fig. 6. Prototype of P-S3BF interface circuit.

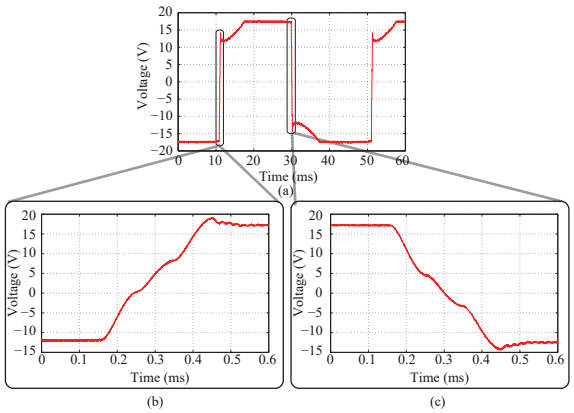

Fig. 7. Experimental results with P-S3BF. (a) Operating waveforms. (b) Upstairs instant. (c) Downstairs instant.

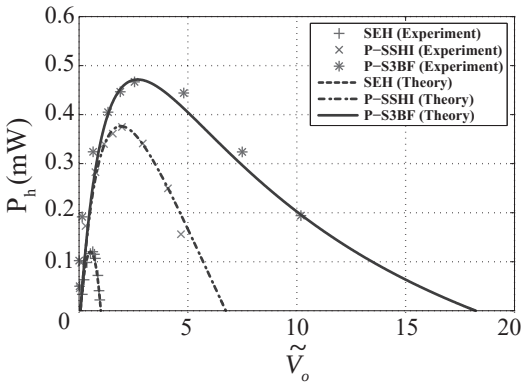

Fig. 8. Harvested power with different interface circuits.

nected to the piezoelectric structure for comparison. The theoretical harvested power is obtained based on the equivalent impedance model. It is expressed as functions of the normalized rectified voltage $\tilde{V_0} = V_0/V_{oc}$. The experimental results are measured for validation. Under constant displacement magnitude excitation, the mechanical effect resulting from the backward coupling can be neglected; therefore, the current source piezoelectric model is valid. The normalized rectified voltage can be changed by connecting different load resistors R_L to the dc output port.

The experimental waveforms are shown in Fig. 7. The voltage profile of P-S3BF is quite similar to that of P-SSHI, except the details in the synchronized instants. Three voltage stairs about the same height are observed in the synchronized instants, which shows a good agreement with the theoretical prediction. V_b can always track the optimal value under different normalized output voltage $\tilde{V_o}$ as expected. Experimental results on harvested power agree with the theoretical one. It shows that P-S3BF outperforms the cutting-edge P-SSHI solution, in terms of maximum harvested power. With the prototyped piezoelectric structure, P-S3BF can increase the harvesting capability by 24.5% compared to P-SSHI, and 287.6% compared to SEH, respectively.

V. Conclusion

This paper introduces a new interface circuit parallel synchronized triple bias flip (P-S3BF) for piezoelectric energy harvesting (PEH) enhancement. The circuit operation principle under steady-state and the transient performance and adaptivity were analyzed in details. The current-routing network with the synchronized triple bias-flip strategy help cut down the power dissipation in bias-flips. The adaptive feature makes P-S3BF a practical solution compared to the state-of-the-art S2BF designs. Experiment on the prototyped PEH system showed that the harvesting capability of P-S3BF outperforms P-SSHI by 24.5% and SEH by 287.6%, which also agrees with the theoretical prediction. Future efforts should focus on the holistic equivalent impedance model for the whole electromechanical PEH system using P-S3BF.

Acknowledgment

The work described in this poster was supported by the grants from National Natural Science Foundation of China (Project No. 61401277).

References

[1] R. Harne and K. Wang, "A review of the recent research on vibration energy harvesting via bistable systems," *Smart Materials and Structures*, vol. 22, no. 2, p. 023001, 2013.

[2] P. Mitcheson, E. Yeatman, G. Rao, A. Holmes, and T. Green, "Energy harvesting from human and machine motion for wireless electronic devices," vol. 96, no. 9, pp. 1457–1486, 2008. [Online]. Available: http://ieeexplore.ieee.org/stamp/stamp.jsp?arnumber=4618735

[3] D. Guyomar and M. Lallart, "Recent progress in piezoelectric conversion and energy harvesting using nonlinear electronic interfaces and issues in small scale implementation," *Micromachines*, vol. 2, no. 2, pp. 274–294, 2011. [Online]. Available: http://www.mdpi.com/2072-666X/2/2/274/

[4] J. Liang, "Synchronized bias-flip interface circuits for piezoelectric energy harvesting enhancement: A general model and prospects," *Journal of Intelligent Material Systems and Structures*, apr 2016. [Online]. Available: http://dx.doi.org/10.1177/1045389X16642535

[5] M. Lallart and D. Guyomar, "Piezoelectric conversion and energy harvesting enhancement by initial energy injection," *Applied Physics Letters*, vol. 97, no. 1, p. 014104, 2010.

[6] J. Dicken, P. Mitcheson, I. Stoianov, and E. Yeatman, "Power-extraction circuits for piezoelectric energy harvesters in miniature and low-power applications," vol. 27, no. 11, pp. 4514–4529, 2012. [Online]. Available: http://ieeexplore.ieee.org/stamp/stamp.jsp?arnumber=6175981

[7] J. Liang and W.-H. Liao, "Impedance modeling and analysis for piezoelectric energy harvesting systems," vol. 17, no. 6, pp. 1145–1157, 2012. [Online]. Available: http://ieeexplore.ieee.org/stamp/stamp.jsp?arnumber=5959210